Wavelength-dependent selective heating and the composite particle design

The guiding principle of our design is that, no matter the orientation of the particle with respect to the beam direction, the wavelength of light should solely determine which hemisphere gets hotter. This is illustrated by the fact that the temperature scale in Figures 3a (500nm) and 3b (800nm) intentionally starts at a value larger than zero (5 degrees). Because TiN appears to have a broader spectral absorption range (as seen in Fig. 2), the corresponding TiN cap (in the composite particle) is intentionally made smaller (i.e. it has less area coverage) than the gold cap. This ensures that for 500nm light, the gold hemisphere will get hotter even when the TiN cap directly faces the light beam. Below we present a case that would not be appropriate for guiding: consider a scenario in which the two caps have the same area coverage and thickness (Supplementary Figure 1). In this case, we observe orientations where wavelength selectivity no longer works: for these orientations (indicated by the checkered area in Sup. Fig. 1) the hemisphere with the TiN cap is hotter than the hemisphere with the gold cap, even for 500nm light. The area coverage corresponds to the spherical angle of $\Omega=6\pi/5$, equal to the spherical angle for the gold cap in the main text.

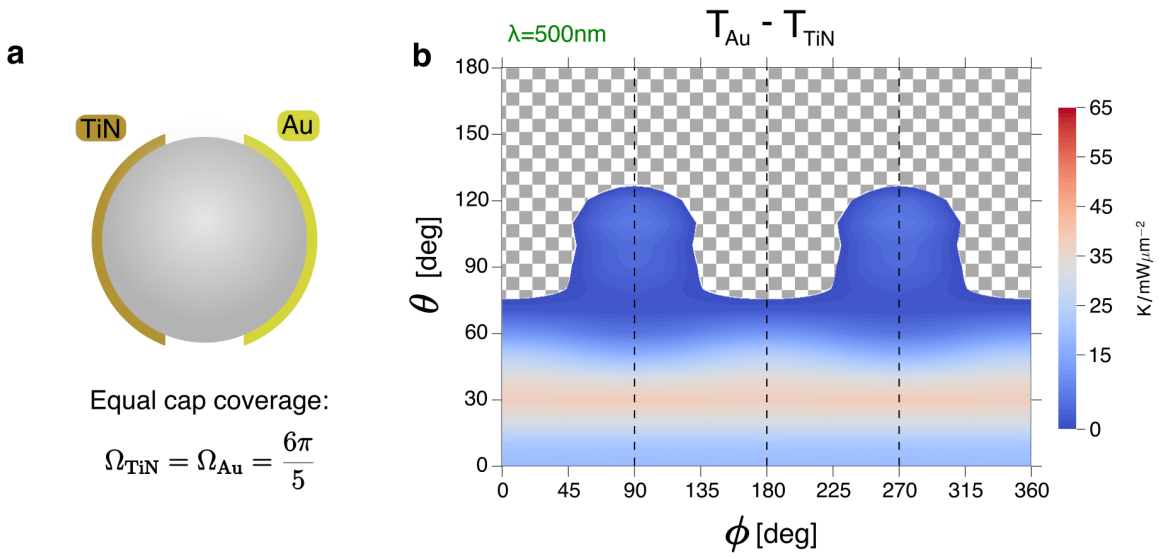

Supplementary Figure 1: Example of a two-cap geometry that is not appropriate for guiding. Temperature pattern (b) for the composite particle design with equal cap coverage (a). Here, λ=500nm; all other parameters are equivalent to those in Fig. 2. Checkered area in (b) corresponds to orientations where the TiN hemisphere is hotter than the gold hemisphere (the color bar values are <0).

Robustness of the composite particle design

In this work, we chose the size of the particle and the thickness of the caps to be similar to the values used in Janus particle experiments in the literature (this allows us to estimate the relationship between the magnitude of the thermophoretic drift and the induced temperature difference). With those two parameters fixed, we vary the cap area coverage to achieve the desired light-induced heating asymmetry. To test the sensitivity of the final design to potential deviations during material deposition, we perturb the geometrical parameters that define the structure. The results are shown in Supplementary Table 1. Unless specified otherwise, the following parameters (default values) are assumed: radius R=500nm, cap thickness d_{cap}=60nm, and the cap coverage areas are given by spherical angles Ω(TiN)=2π/5 and Ω(Au)=6π/5. For these variations, we calculate the resulting temperature difference between the two hemispheres, for both the 500nm and the 800nm light. As in Figure 2, these are normalized to the incident beam intensity (here θ=90°, ϕ=0°).

		λ=500nm	λ=800nm
Parameter	Variation	$\boldsymbol{T}$(Au) - $\boldsymbol{T}$(TiN) [K/mWμm^{-2}]	$\boldsymbol{T}$(TiN) - $\boldsymbol{T}$(Au) [K/mWμm^{-2}]
Default values	None	39.3	32.7
R=500nm	-10%	54.6	20.1
	+10%	32.0	71.8
d_{cap}=60nm	-10%	40.6	25.0
	+10%	38.5	40.0
Ω(TiN)=2π/5	-10%	43.1	28.6
	+10%	35.6	36.5
Ω(Au)=6π/5	-10%	36.9	34.3
	+10%	41.3	31.7

Supplementary Table 1: Robustness of the composite particle design to variations in geometrical parameters.

We observe that the variations in geometrical parameters (of ±10%) introduce no qualitative change in the heating patterns: primarily, the sign of the temperature difference is unchanged. The temperatures appear to be most sensitive to the overall particle size (which is the largest dimension in the system, governing the scattering and the heat distribution in the entire structure), with much reduced sensitivity to other parameters. This implies that deviations in the caps during fabrication should not significantly alter the behavior predicted by the model.

Analysis of the cap edges

In problems of electromagnetics, sharp edges or pointy corners may lead to highly intense and concentrated electric fields. Consequently, such enhanced fields could become “hot spots”, and sources of particularly strong, localized, heating. If such edge effects were to significantly affect the heating of our

composite nanoparticle, it could complicate the fabrication of the particle, resulting in a process that is especially sensitive to the deposition of different cap materials.

However, we show that this is not the case in our design. By numerically simulating three different types of cap edges, we observe no relevant differences in the resulting heating patterns. The three types of edges are shown in Supplementary Figure 2, and include sharp angles (a), perpendicular faces (b), as well as filleted, smooth corners (c).

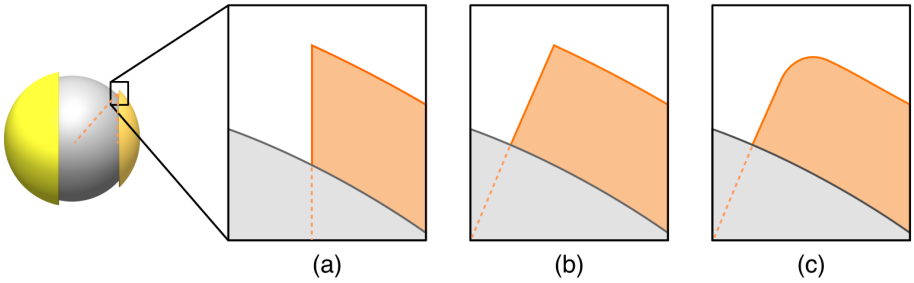

Supplementary Figure 2: Evaluating different types of cap edges and their effect on particle heating. The three figures are zoomed-in views of the three types of edges. Exact simulations of these representative designs demonstrate that cap edges have no significant influence.

We quantify the three cases by comparing the relevant temperatures in the system: the average temperature of the hemisphere with the gold cap and the average temperature of the hemisphere with the TiN cap. In finite-element simulations, we found that these temperatures differ by less than a percent for the three different types of edges, a discrepancy that could also be attributed to the finite meshing of the geometry of the system (particularly for the smooth filleted corner). Similarly, the variation in the optical pressure is small.

Equations of translational and rotational dynamics

In equations 1 and 2 of the main text, M_{opt}, F_{opt} refer to the optical torque and force (radiation pressure). In our case (Fig. 1), we theoretically estimate (from the Maxwell stress tensor) the radiation pressure force to be ~4pN/mWμm^{-2}, with some variation depending on the particle orientation. It was experimentally reported, however, that the thermophoretic drift force was stronger than the radiation pressure force for the same-size, single-coated, Janus particle[22]. Still, we note that radiation pressure is easily eliminated experimentally, for example, by considering counter-propagating beams, or motion confined to a plane perpendicular to illumination. Hence, in the same way as was previously done in the literature[22,23], we focus on the thermophoretic drift and exclude the radiation pressure from subsequent analysis.

Conditions for effective bi-directional thermophoretic particle guiding

The relative strength of the induced thermophoretic drift to the translational diffusion has two extremes. On one hand, for weak light intensities, the translational diffusion dominates over the thermophoretic drift, and the particle is very weakly guided. On the other, for high intensities, the drift the particle experiences can be strong. A strong thermophoretic drift—provided it is in the right direction—is

desirable for traversing large distances, but can hinder the ability to accurately approach a target. To characterize the potential of bi-directional thermophoretic guiding to localize a particle to a specific point in space r_0, we evaluate the quantity $\chi^2 = \left\langle |r - r_0|^2 \right\rangle$, when the guiding algorithm is turned "on", with the goal of bringing the particle to r_0. The quantity χ depends on the beam intensity as well as the guiding time step.

In Supplementary Figure 3, we show this dependence for various parameter values (for the same composite particle shown in Fig. 1, in water). When the thermophoretic drift ($\boldsymbol{U}_{th}$) dominates over translational diffusion, the quantity χ is independent of time – we call this the regime of guided/localized dynamics. We observe this behavior for strong enough light intensities: these data points are shown as circles in Sup. Fig. 3. An appropriate combination of source intensity and guiding time-step would confine a particle to an average distance from the target that is just slightly larger than the particle itself (χ/a~1.2), allowing for a very accurate approach to target.

On the other hand, when the source intensity is zero, the particle simply performs a random walk, and the average distance increases in time as $\sqrt{6D_{tr}t}$, where D_{tr} is the translational diffusion coefficient (approximately $0.5\mu m^2/s$, for a 1μm particle in water). This is shown in the leftmost part of Sup. Fig. 3 (gray triangles), evaluated at times t_1=25s, t_2=50s, t_3=100s. In between these two extremes is the regime of drifting dynamics: here the source intensity is not strong enough to permanently confine a particle, but the particle drift (χ/a) can still be made much slower than a pure random walk. These are represented as (purple) triangles (for times t_1=25s, t_2=50s, t_3=100s).

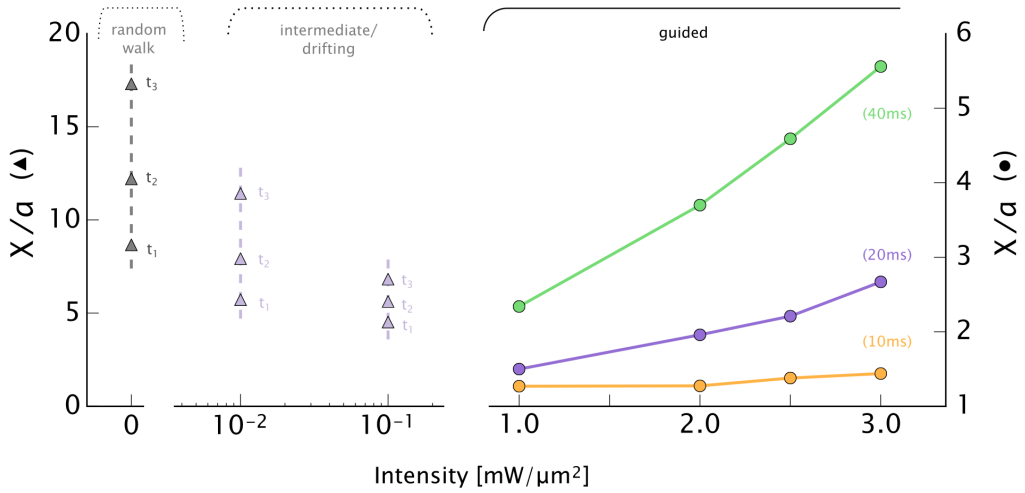

Supplementary Figure 3: Conditions for effective guiding: guided regime (circles and solid lines) where the guiding time-step τ_1 is varied (τ_1=10, 20, 40ms), pure random walk regime (left-most, gray triangles; zero intensity) at times t_1=25s, t_2=50s, t_3=100s, and the intermediate regime of weak guiding (purple triangles, same t_1, t_2, t_3; here τ_1=20ms).

Guiding of multiple particles

Our focus so far has been on single-particle guiding. Nevertheless, a similar approach could in principle be used to manipulate and transport many such asymmetric particles. Consider an ensemble of N particles equivalent to that of Fig. 1 and initially oriented in random directions. For simplicity, we assume the particles do not interact with one another (e.g. a sufficiently dilute solution) and we focus on their motion along one of the axis (e.g. a flow in a tube). The same axis (call it the X axis) is perpendicularly illuminated by light of two wavelengths (λ_1=800nm and λ_2=500nm) in a periodic fashion, as shown in Supplementary Figure 4a. This illumination pattern creates a periodic array of regions, shown in red (for 800nm light) and green (for 500nm light). We assume equal light intensity in both types of regions.

In the beginning (t=0), all N particles are in the vicinity of X=0 (and have some distribution in the other two dimensions, which does not affect the dynamics). If the intensity of light were zero (or the same wavelength of light were used everywhere), the particles would on average drift in equal numbers to the left (X<0) and to the right (X>0). The purpose of the periodic pattern of illumination is to temporarily localize the particles. Specifically, the interfaces between the regions of different wavelength serve as barriers to particle motion. For example, consider a particle oriented in such a way that 500nm light provides a preferential thermophoretic drift to the right. As that particle crosses the green-red interface into the "red" region, it is now driven backwards, and ultimately confined to the interface itself. This localization to a specific interface is, of course, temporary: the particle orientation diffuses with the characteristic rotational diffusion time (τ_{rot}). Nevertheless, by translating the illuminated pattern to the chosen direction, the localization points are also shifted, without losing too many of the particles trapped in the boundaries between the alternating regions.

Supplementary Figure 4 illustrates the guiding of multiple particles. The N particles ($N=10^3$) all start at X=0 (see zoom-in panel in the same figure), and the objective is to move them towards the target to the right (X>0). To achieve this goal, we introduce an illumination pattern of spatial period Λ_P, also moving to the right at the rate of v_P. The figure shows the histogram of particle locations at different times t =0, τ_{rot}, $10\tau_{rot}$, $50\tau_{rot}$, and the corresponding average position of the ensemble $\langle X \rangle$. We observe that it is indeed possible to guide many particles, and to do so long after the initial particle orientations have been lost (i.e. for times significantly longer than τ_{rot}). Below, I=2.5mW/μm^2, Λ_p=20μm, and v_P=25μm/s. Of course, a different choice of parameters (e.g., wider areas of "red" and "green") would change the properties and quality of guiding, leaving much space for further optimization.

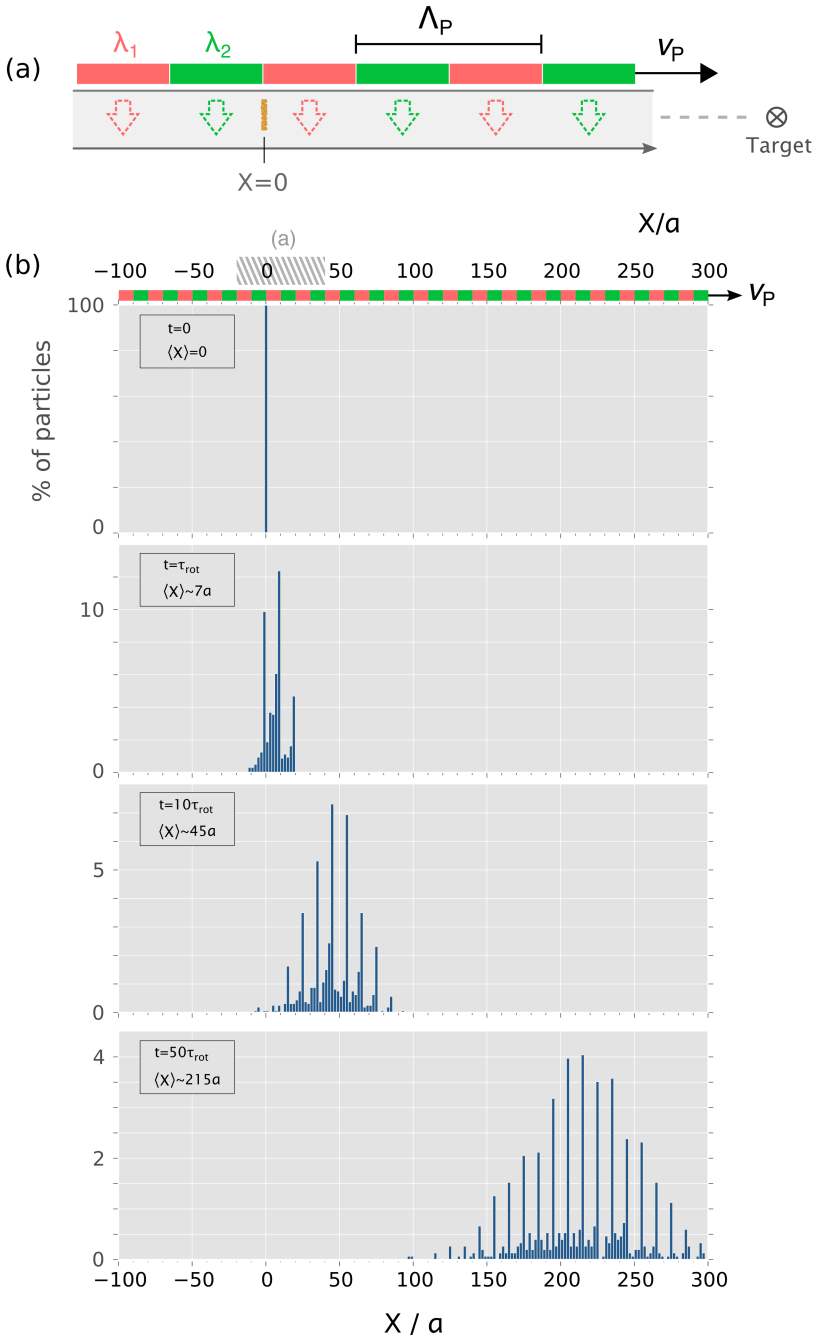

Supplementary Figure 4: A scheme for guiding multiple particles. (a) Sketch of a periodic illumination pattern along the X-axis (period Λ_p) moving to the right (at the rate v_P). Initially (t=0), all particles ($N=10^3$) are at X=0. Subsequently (b), due to thermophoresis the particles preferentially drift to the right (towards the target), partially confined at the boundaries between regions of different illuminating wavelength (hence the spikes in the histogram). Insets: the average ensemble position at different times (in multiples of the rotational diffusion time τ_{rot}). The particles and the surrounding medium are identical to those of the main text. The shaded area around X=0 in (b) is shown zoomed-in (a).